Carbohydrate Polymers 94 (2013) 292–300

Contents lists available at SciVerse ScienceDirect

Carbohydrate Polymers

journal homepage: www.elsevier.com/locate/carbpol

Supramolecular complexes of maltodextrin and furosemide polymorphs: a new approach for delivery systems

Claudia Garnero[a], Ana Karina Chattah[b], Marcela Longhi[a,*]

[a] Departamento de Farmacia, Facultad de Ciencias Químicas, Universidad Nacional de Córdoba, Ciudad Universitaria, X5000HUA Córdoba, Argentina
[b] Facultad de Matemática, Astronomía y Física and IFEG (CONICET), Universidad Nacional de Córdoba, Ciudad Universitaria, X5000HUA Córdoba, Argentina

ARTICLE INFO

Article history:
Received 7 November 2012
Received in revised form 18 January 2013
Accepted 19 January 2013
Available online xxx

Keywords:
Furosemide
Polymorphism
Maltodextrin
Solubility
Complex characterization

ABSTRACT

We present new supramolecular complexes of two different solid forms of furosemide (I or II) with maltodextrin, in order to explore their application as delivery systems improving the bioavailability of the drug. The complexation in solution was evaluated by ^{1}H nuclear magnetic resonance experiments and phase solubility studies. The products in solid state were exhaustively characterized by using spectroscopic techniques (^{13}C solid state nuclear magnetic resonance, infrared, scanning electron microscopy, X-ray powder diffractometry) and thermal analysis. ^{1}H relaxation times experiments gave further support in distinguishing the new solid forms. Dissolution studies in simulated gastric fluid showed that both supramolecular complexes presented significant increase in the dissolution, while the corresponding physical mixtures exhibited the most discriminating conditions between the furosemide forms I and II. Our results suggest the enhancement of the solubility and the dissolution of furosemide in the new complexes, making them promising candidates for the preparation of alternative matrices in oral pharmaceutical formulations.

1. Introduction

It is well-established that pharmaceutical solids can exist in several polymorphic forms having very varied physical and mechanical properties, with resulting differences in the activity of the drug molecules (Brittain, 2009; Snider, Addicks, & Owens, 2004). As a drug is affected by the properties of the solid form, experimentally obtained information about the solid-state behavior during production and storing, and knowledge of the solubility and dissolution conditions are very important to be able to select the solid form with the optimal characteristics for the intended use (Hilfiker, 2006).

Furosemide (FUR, Fig. 1) is widely applied as a strong loop diuretic in the pharmacotherapy of edematous states associated with cardiac, renal, and hepatic failure and the treatment of hypertension (Sweetman, 2009). Although seven polymorphic forms have been described and characterized for this compound (four true polymorphs (I, II, III, IV), two solvates (IV–DMS and V–dioxane) and one amorphous form [Bauer et al., 2002; Beyers, Malan, van der Watt, & de Villiers, 2000; Doherty & York, 1988; Latosinska, Latosinska, Medycki, & Osuchowicz, 2006; Matsuda & Tatsumi, 1990; Pudipeddi & Serajuddin, 2005]), polymorph-dependent bioavailability has not been reported to date. It is known that FUR is practically insoluble in water. In humans, FUR is absorbed from the upper gastrointestinal tract following dissolution in the stomach. Its bioavailability has been reported to be about 60–70% (Sweetman, 2009), but the rate and extent of absorption are subject to large inter- and intra-subject variabilities. In addition, absorption following oral administration is influenced by the dosage form, underlying disease processes and by the presence of food (Ponto & Schoenwald, 1990).

An approach to increase the water solubility, stability, and bioavailability of drugs is the formation of complexes with modified starches as cyclodextrins, calyx[*n*]arenes and maltodextrins (MDs) (Brewster & Loftsson, 2007; Corralo Spada, Zapata Noreña, Ferreira Marczak, & Tessaro, 2012; Munoz-Celaya et al., 2012). In particular, recently MD based systems have been used successfully for drug delivery (Gurrapu, Jukanti, Bobbala, Kanuganti, & Jeevana, 2012; Kumar, Subbarao Murthy, & Sahu, 2012). MDs are products obtained from the partial hydrolysis of food grade starch with suitable acids and/or enzymes (Reineccius, 1989; Shahidi & Han, 1993). The D-glucose units are primarily linked by α-(1,4) bonds, but there are also branched segments linked by α-(1,6) bonds (Shahidi & Han, 1993). MDs differ in average molecular size and are classified by their dextrose equivalent (DE) values, defined as the percentage of reducing sugars calculated as glucose on a dry substance basis (Wang & Wang, 2000). Normally, MDs are defined as having a DE value of less than 20 and, depending on this value, they have distinct physicochemical properties, such as

* Corresponding author. Tel.: +54 351 4334127; fax: +54 351 4334127.
E-mail addresses: mrlcor@fcq.unc.edu.ar, mrlonghi@gmail.com (M. Longhi).

0144-8617/$ – see front matter © 2013 Elsevier Ltd. All rights reserved.
http://dx.doi.org/10.1016/j.carbpol.2013.01.055

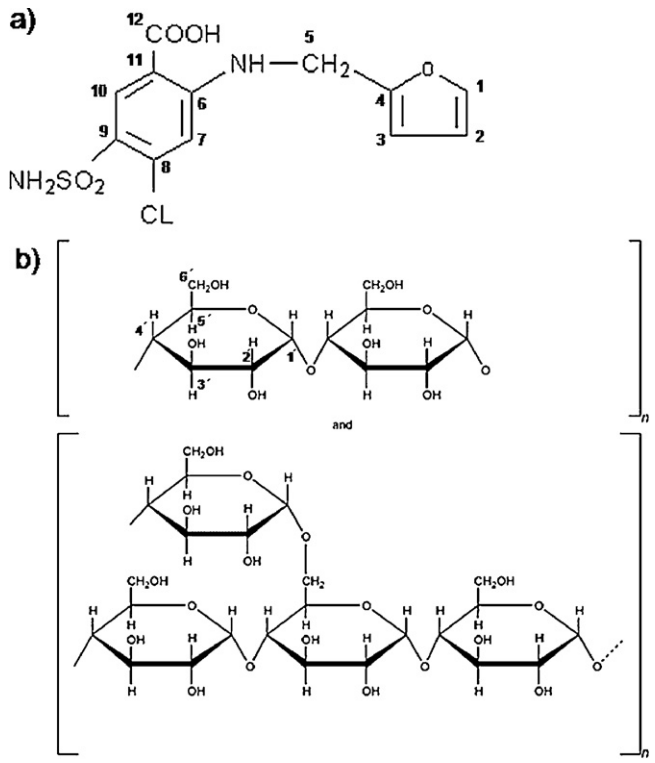

Fig. 1. Chemical structure of (a) FUR and (b) MD, showing the carbon and proton numbering used in the NMR spectra.

solubility, freezing temperature and viscosity (Dokic, Jakovljevic, & Dokic-Baucal, 1998; Dokic-Baucal, Dokic, & Jakovljevic, 2004). Their typical structures are shown in Fig. 1.

The MDs are endowed with the capability of complexation to various classes of compounds, with the host-guest one being the most common interaction for starch derivatives. The conformational change from a flexible coil to a helix form in the presence of a guest, which depends on the size of the complexing molecules, is believed to be essential for interactions to occur. Internally, the helical structure is hydrophobic, as in the cyclodextrin cavity, but MDs have considerably more flexible entities than cyclodextrins (Soini, Stefansson, Riekkola, & Novotny, 1994).

In previous reports, several strategies have been developed to increase the solubility and/or the dissolution rate of FUR, for example using cyclodextrins (Vlachou & Papaioannou, 2003), calix[*n*]arenes (Bayrakci, Ertul, & Yılmaz, 2012) and particle size reduction as well as formation of solid dispersions (De Zordi et al., 2012). However, these studies do not refer about the polymorphism of this drug. Because it is of great importance to select a proper polymorph and to control its polymorphic transformations, we focused our work on preparing and characterizing new supramolecular systems of FUR polymorphs I and II with MD DE17. The aim of these complexes was to enhance the low permeability and the solubility of FUR, which are the two critical factors responsible for its poor and highly variable human bioavailability. Complexation in solution and solid state was studied using solubility analysis, solution and solid state Nuclear Magnetic Resonance (ssNMR), Fourier-transform infrared spectroscopy (FT-IR), differential scanning calorimetry (DSC), thermogravimetric analysis (TGA), scanning electron microscopy (SEM), and X-ray powder diffraction (XRPD). In addition, ^{1}H spin lattice relaxation time measurements were also carried out in solid state. In order to investigate the potential application of the supramolecular complexes as new delivery systems that enhance the bioavailability of the drug, dissolution tests were used to correlate the performance between the polymorphic forms and the complexes.

2. Materials and methods

2.1. Chemicals and reagents

Furosemide was provided by Parafarm (Argentina), Maltodextrin (DE17) was given by Todo Droga (Argentina), and D_2O (deuterium content 99.9%) was obtained from Aldrich® (USA). All other chemicals were of analytical grade. A Millipore Milli Q Water Purification System (Millipore, Bedford, MA, USA) generated the water used in these studies.

2.2. Obtaining two polymorphic forms of furosemide

The two polymorphic forms of FUR, I and II, were prepared as reported by De Villiers, van der Watt, and Lotter, 1992. Form I was recrystallised from a hot saturated solution of FUR in methanol, which was allowed to stand at room temperature. Form II was obtained from an acetone solution, which was evaporated to dryness at 25 °C under reduced pressure in a rotary evaporator. The resulting crystals were collected and dried in vacuo at room temperature.

2.3. Solubility studies

The effects of MD with DE 17 on the solubility of FUR polymorphs were studied at 25.0 ± 0.1 °C in aqueous and buffered aqueous solutions of pH 2.0, and at 37.0 ± 0.1 and 45.0 ± 0.1 °C in solutions of pH 2.0. The solubility measurements were performed according to the method of Higuchi and Connors (1965). An excess of FUR forms I or II, was added to solutions containing increasing concentrations of MD ranging from 0.50 to 10.00% (w/v), with FUR, in the absence of MD, being used to determine the intrinsic solubility. The suspensions were sonicated for 15 min (ULTRASONIC LC 30 H Elma) and then placed for 72 h in a constant temperature water bath [Haake DC10 Thermostat (Haake, Paramus, NJ, USA)]. These suspensions were sonicated at several time intervals, and after the equilibrium was reached, the remaining solid FUR was removed by filtration through a 0.45 μm membrane filter (Millipore, USA). The clear solutions were suitably diluted and analyzed by UV–Vis Spectrophotometry (SHIMADZU UV-160A spectrophotometer) at λ = 274 nm.

2.4. Solid sample preparations

Solid-state systems of FUR polymorphs I and II in equimolar ratio with the MD were prepared as following.

2.4.1. Kneading method (KN)

The FUR I:MD (KN I) and FUR II:MD (KN II) systems were prepared by weighing accurately appropriate amounts of MD and then transferring them to a mortar. An ethanol–water (50:50, v/v) mixture was added to the MD powder and the resultant slurry was kneaded for about 10 min. For each system, the corresponding FUR polymorph was added in small portions with the simultaneous addition of solvent in order to maintain a suitable consistency. This slurry was kneaded thoroughly for about 30 min, and the resultant paste was dried in vacuo at 40 °C for 48 h, protected from light.

2.4.2. Physical mixture (PM)

Physical binary mixtures of FUR I:MD (PM I) and FUR II:MD (PM II) were prepared by blending the corresponding components uniformly in a mortar.

2.5. Solution NMR

^{1}H NMR spectra of FUR and the combination of FUR and MD were recorded in D_2O. In addition, ^{13}C NMR, heteronuclear single quantum correlation with distortion enhancement by polarization transfer (^{1}H–^{13}C HSQC-DEPT) and heteronuclear multiple bond correlation (HMBC) experiments were realized for FUR. A small amount of methanol (<1 mM) was added to the FUR solutions due to its poor solubility in D_2O, and the concentration of the components was 15 mM. All experiments were performed on a Bruker® Avance II 400.16 MHz High Resolution Spectrometer equipped with a Broad Band Inverse probe (BBI) and a Variable Temperature Unit (VTU). The spectra were obtained at 298 K using 5 mm sample tubes. The chemical shifts (δ) were reported as ppm, and the residual solvent signal (4.80 ppm) was used as the internal reference. Induced changes in the ^{1}H NMR chemical shifts ($\Delta\delta$) for FUR caused by its interaction with MD, were calculated according to the following equation:

$$\Delta\delta = \delta_{\text{complex}} - \delta_{\text{free}} \quad (1)$$

2.6. Solid state NMR (ssNMR)

High resolution solid state ^{13}C spectra of FUR I and II, the MD and the systems KN I, KN II, PM I and PM II, were recorded with the ramp cross polarization/magic angle spinning (CP-MAS) sequence, with proton decoupling during acquisition (Harris, 1994). All ssNMR experiments were performed at room temperature in a Bruker Avance II spectrometer operating at 300.13 MHz for protons and equipped with a 4 mm MAS probe. The operating frequency for carbons was 75.46 MHz. Glicine was used as an external reference for the ^{13}C spectra and for setting the Hartmann–Hahn matching condition in the CP. Spectra were recorded with 2000 or 3000 scans to obtain an adequate signal to noise ratio. The contact time during CP was 2 ms and recycling times of 5 and 10 s were used. The SPINAL64 pulse sequence was used for decoupling during acquisition, with the proton field H_{1H} satisfying $\omega_{1H}/2\pi = \gamma_H H_{1H}/2\pi = 78$ kHz (Khitrin, Fujiwara, & Akutsub, 2003). The spinning rate for all the samples was 10 kHz. Quaternary carbon and methyl group edition spectra were recorded for FUR I and II. These spectra were acquired with the non-quaternary suppression (NQS) sequence (Harris, 1994).

^{1}H spin–lattice relaxation times in the laboratory frame (T_1) measurements were carried out for all the solid samples in static conditions with an inversion-recovery (IR) pulse sequence, using recovery times τ of between 10 μs and 300 s with a recycling delay of 160 s.

2.7. FT-IR spectroscopy

The FT-IR spectra were recorded on a Nicolet 5 SXC FT-IR Spectrophotometer (Madison, WI, USA). The potassium bromide disks were prepared by compressing the powder.

2.8. Thermal analysis (DSC and TGA)

The DSC curves of the samples were produced with a DSC TA 2920, and the TGA curves were recorded on a TG TA 2920. The samples of 1–3 mg were placed in aluminum hermetic pans, and the experiments were carried out under a nitrogen gas flow, at a heating rate of 10 °C/min over a temperature range of 25–300 °C.

2.9. SEM

Microscopic morphological structures of the raw materials and the solid-state systems were investigated and photographed using a scanning electron microscope LEO Model EVO-40 XVP. The samples were fixed on a brass stub using double-sided aluminum tape. To improve the conductivity, samples were gold-coated under vacuum by employing a sputter coater PELCO Model 3. The magnification selected was sufficient to appreciate in detail the general morphology of the samples under study.

2.10. XRPD

X-ray powder diffraction patterns of the samples were recorded using a Philips PW1710 diffractometer, with Ni filtered Cu Kα radiation. Measurements were taken from 2 to 40° (2θ) at steps of 0.05°, a voltage of 45 kW and a current of 30 mA for the generator.

2.11. Dissolution study

The dissolution tests were carried out at 37 °C using the USP XXX paddle apparatus (Hanson SR II 6 Flask Dissolution Test Station, Hanson Research Corporation, Chatsworth, CA, USA) with three replicates. The dissolution medium was simulated gastric fluid (pH 1.2) without enzymes prepared according to USP30. Testing was conducted on samples of FUR forms I and II, and also for the systems KN I, KN II, PM I and PM II. Suitable quantities of each powder containing 50 mg of drug were compressed using a hydraulic press at an appropriate force to obtain discs which would not disintegrate under the test conditions. The discs were immersed into 500 ml of the dissolution medium and agitated at 50 rpm. Samples were collected at prearranged time intervals, with replacement, before being filtered and adequately diluted with dissolution media. The amount of dissolved drug in the samples was analyzed spectrophotometrically at 274 nm. Cumulative percentages of the drug released from the discs were calculated.

3. Results and discussion

3.1. Phase solubility analysis

The effect of MD on the solubility of FUR I and II was investigated at 25.0 ± 0.1 °C in aqueous solutions. In order to determine the influence of temperature, the phase solubility diagrams were determined at 25.0 ± 0.1, 37.0 ± 0.1 and 45.0 ± 0.1 °C in buffered solutions of pH 2.0, thus simulating the gastric fluid where the drug molecule is unionized. The phase solubility diagrams were obtained by plotting the changes in FUR solubility as a function of MD concentration (see Supplementary data).

The interactions of the FUR I:MD and FUR II:MD systems, both in aqueous and buffer solutions at 25.0 ± 0.1 °C, displayed typical A_L type solubility curves (Brewster & Loftsson, 2007), indicating the formation of soluble binary complexes of a presumably 1:1 stoichiometry. The apparent stability constant (K_C) values, shown in Table 1, were estimated from the slope of the initial linear portion of the diagrams and the intrinsic solubility of each polymorph (S_0) according to the following equation:

$$K_C = \frac{\text{slope}}{S_0(1 - \text{slope})} \quad (2)$$

On analyzing the effects of pH, it could be observed that the value of K_C for FUR I:MD was higher in aqueous solutions. These results reveal that ionized FUR I exhibited a higher affinity for the host than the neutral species. However, FUR II showed the same value of K_C in both solvents, indicating that the ionization did not affect the interaction of this polymorph with MD. The solubility of both systems was higher in water, because of the combined effect of the complex formation and the existence of the drug as an ionized species.

Table 1
Summary of solubility studies.

Temperature	FUR I:MD system			FUR II:MD system		
	S_0 (μg/mL)	S_{max} (μg/mL)	K_c (M^{-1})	S_0 (μg/mL)	S_{max} (μg/mL)	K_c (M^{-1})
Aqueous solution						
25.0 ± 0.1 °C	35.6	79.1	193	27.4	50	167
Buffer solution						
25.0 ± 0.1 °C	4.4	13.7	156	6.1	15.8	167
37.0 ± 0.1 °C	6.1	24.5	–	4.4	30.2	–
45.0 ± 0.1 °C	13.1	25.4	–	15.2	26.4	–

The profiles obtained with the buffer solution at 37.0 ± 0.1 and 45.0 ± 0.1 °C were characteristic of A_N type diagrams (Brewster & Loftsson, 2007), demonstrating a negative deviation from linearity as a function of MD concentration, and indicating that the solubilizing capacity was less effective at higher temperatures. This behavior may have originated from both an alteration in the effective nature of the solvent and a self-association of MD at higher concentrations, thus affecting the apparent degree of complexation.

These studies also revealed different solubility behaviors of both polymorphs. Whereas at 25 °C polymorph I had the highest intrinsic solubility in water, in buffer solution of pH 2, polymorph II was the more soluble. In addition, it can be noted that the apparent solubility of each FUR polymorph was significantly increased upon complexation with MD, as shown in Table 1. In buffer solution, FUR I solubility increased as a function of MD concentration and with a rise in temperature. However, the FUR II system showed the highest solubility value at 37.0 ± 0.1 °C.

3.2. Nuclear magnetic resonance (NMR) experiments

Heteronuclear single quantum correlation with distortion enhancement by polarization transfer (^1H–^{13}C HSQC-DEPT) and heteronuclear multiple bond correlation (HMBC) experiments were carried out to obtain the full assignment of the FUR ^1H spectrum (not shown). The ^1H NMR spectra were recorded to evaluate the changes in the chemical shifts ($\Delta\delta$) of FUR after forming MD complexes, and the corresponding $\Delta\delta$ are displayed in Table 2 (see proton numbering in Fig. 1). It can be observed that most of the FUR protons were influenced by the presence of MD. Deshielding was observed for H1, H2, H5 and H10, while H3 and H7 showed shielding effects. These shifts suggest the establishment of van der Waals interactions and the proximity of atoms rich in π electrons such as glycosidic linkage oxygens, respectively. It is important to note that H7 revealed the greatest displacement in the binary system with respect to the pure drug. This behavior indicates that the FUR benzene ring containing the sulphonamide group was involved in the interaction between FUR and MD, thus confirming the formation of a supramolecular complex in solution.

Table 2
^1H NMR chemical shifts corresponding to FUR free and in the presence of the binary system FUR:MD.

Proton	δ_0 [a]	δ_C [b]	$\Delta\delta$ [c]
H1	7.4993	7.5244	0.0251
H2	6.4476	6.4614	0.0138
H3	6.3999	6.3886	−0.0113
H5	4.5284	4.5441	0.0157
H7	7.0622	7.0057	−0.0565
H10	8.3943	8.4282	0.0339

[a] δ free.
[b] δ complex.
[c] $\Delta\delta = \delta_C - \delta_0$.

3.3. Solid state characterization

3.3.1. Solid state NMR

The solid state ^{13}C CP-MAS spectra for FUR I and II are shown together with their NQS spectra in Fig. 2(a–d). The corresponding carbon chemical shifts can be seen in the Supplementary data. The assignments were made by taking into account the quaternary carbon edition spectra and by comparing with solution ^{13}C NMR and solid state spectra previously reported (Doherty & York, 1988). The ^{13}C CP-MAS spectrum of MD (Fig. 2(e)) exhibited broad signals that were assigned based on the solution NMR spectrum.

It was possible to identify the polymorphs I and II of FUR from their ^{13}C solid state spectra, due to several sharp resonances that could be distinguished in each case. Consider, for example, the shift of 1.4 ppm in C12, a signal around 148 ppm in FUR II, and 117.6 and 154 ppm in FUR I. Note that there are two resonances for some carbons in FUR I (C6, C9, C10, C11), providing evidence of more than one molecule in the unit cell. In contrast, the broad peaks in the ^{13}C spectrum of MD suggest an amorphous material with resonances of 400 Hz wide. It is interesting to note that the signals in the MD spectrum (inside the region between 58 and 107 ppm) are separated from those of the FUR spectra (in the region between 105–176 ppm and 42 ppm).

Fig. 3 displays the ^{13}C CP MAS spectra of the complexes KN I (a) and KN II (b), the corresponding physical mixtures PM I (c) and PM II (d), and the pure drugs FUR I (e) and FUR II (f). Comparing the KNs spectra with those of the corresponding PMs, it can be seen some differences in the relative intensities of the broad signals found in the region between 58 and 107 ppm. This fact indicates that the KNs are new solid forms with an amorphous character. The presence of sharp signals in the region 105–176 ppm, in the chemical shifts belonging to FUR, indicates that there is a certain amount

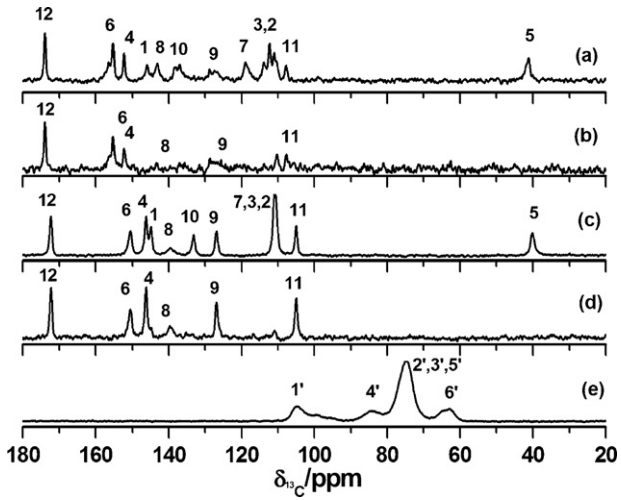

Fig. 2. ^{13}C CP-MAS spectra of (a) FUR I, (c) FUR II and (e) MD. NQS spectra of: (b) FUR I and (d) FUR II. The numbering corresponds to those in Fig 1.

of pure drug without interacting to MD. On the other hand, the amorphous character of the complexes prevented to observe the corresponding part of FUR interacting to MD. Both complexes and the PMs presented only signals of FUR I. Then a phase conversion occurred from FUR II to I in the mixing process of preparation of KN II and PM II. Comparing KN I with KN II, the spectra look very similar, nevertheless there are differences in the relative intensity of the signals belonging to the range of 100–180 ppm, making them, distinguishable spectra.

To obtain additional information on the interaction between FUR polymorphs and MD, we measured continued relaxation time experiments measuring ^{1}H–T_1. The spin diffusion process tends to average the spin lattice relaxation times of the different protons in a sample to a single value. This average is usually complete when protons belong to the same phase domain, whereas relaxation times of different domains in heterogeneous samples can be averaged or not, depending on the dimensions of the different domains. This allows information to be obtained on the mixing degree of the different domains on a 100 A scale (Geppi, Guccione, Mollica, Pignatello, & Veracini, 2005).

To determine the ^{1}H–T_1 values from the IR experiments in each compound, the broad ^{1}H spectrum was integrated. Then, the behavior of ^{1}H magnetization as a function of the recovery time was fitted using one or two relaxation times. Table 3 displays the values of T_1 for all the compounds. The high crystallinities of FUR I and FUR II led to very long values for T_1 (45.8 and 35.2 s) in a very different order of magnitude than MD. For the measurements of the PMs, two relaxation times were obtained with values close to those belonging to each pure component. One of these was very close to MD ^{1}H–T_1, with the other being similar to the FUR polymorph used to prepare the physical mixture involved. In turn, the measurements in the KNs gave two values of relaxation times, with the short T_1 values (5 s for KN I and 4 s for KN II) being different to that corresponding to MD. This fact provides evidence of the presence of a new solid form originating from the molecular interaction between the corresponding FUR polymorph and MD, which can be identified from its dynamical properties being different from its precursors.

Table 3
^{1}H–T_1 values obtained by fitting the experimental data of ^{1}H magnetization vs recovery time with one or two parameters for the relaxation times. Errors are within 7%.

	T_1 (s)	
MD	2.26	
FUR I	45.8	
FUR II	35.2	10
FUR I:MD system		
PM I	38.9	2.31
KN I	48.7	5.00
FUR II:MD system		
PM II	27.4	2.36
KN II	31.4	4.00

Note that the long T_1 value in each case corresponded to a certain amount of free FUR that remained in the complex, as was observed spectroscopically.

3.3.2. FT-IR

In order to identify the individual polymorphic forms of FUR, the characteristic FT-IR bands were examined (Fig. 4(a)), with the main differences between the polymorphs being seen in the 3400–3200 cm^{-1} and 1350–1100 cm^{-1} zones. The FT-IR spectrum of FUR I was characterized by bands at: 3398 and 3284 cm^{-1} (sulphonamide NH stretch), 3352 cm^{-1} (secondary amine NH stretch), and 1322 cm^{-1} and 1141 cm^{-1} (S=O stretch), while FUR II exhibited bands at: 3345 cm^{-1} (secondary amine NH stretch), 3251 cm^{-1} (sulphonamide NH stretch), and 1337 cm^{-1} and 1169 cm^{-1} (S=O stretch). The observed spectral features agreed with those reported previously (Doherty & York, 1988; Matsuda & Tatsumi, 1990).

As shown in Fig. 4(b), in the FT-IR spectrum of KN I, the band assigned to the S=O stretch was shifted to the higher frequency of 1148 cm^{-1}. In addition, the bands corresponding to the C=O (1671 cm^{-1}) and Cl (581 cm^{-1}) vibrations were shifted to 1674 and 575 cm^{-1}, respectively. From these events, we suggest that the

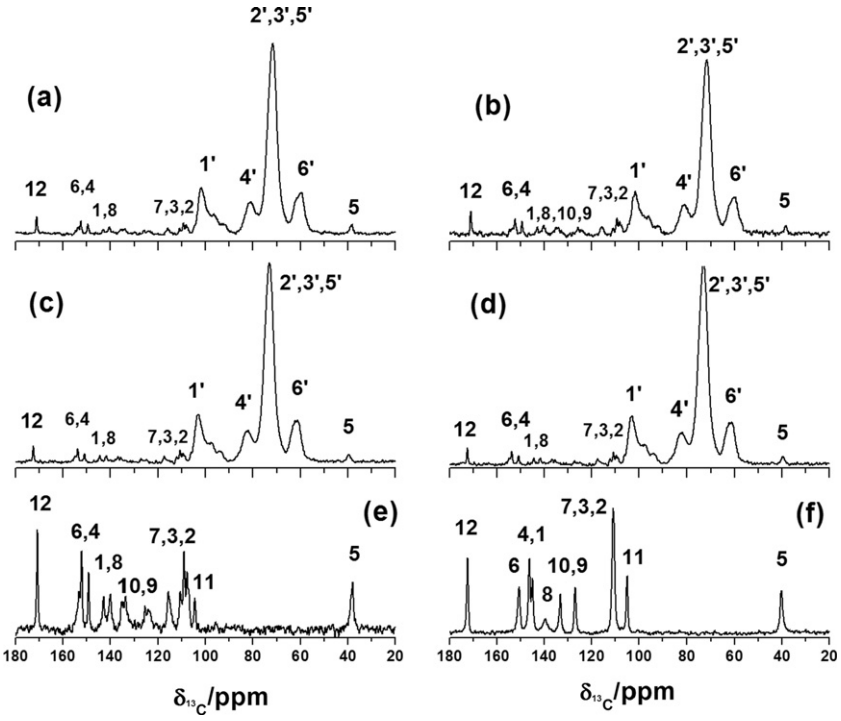

Fig. 3. ^{13}C CP-MAS spectra of (a) KN I, (b) KN II, (c) PM I, (d) PM II, (e) FUR I and (f) FUR II. The numbering has been included for visible signals in the spectra.

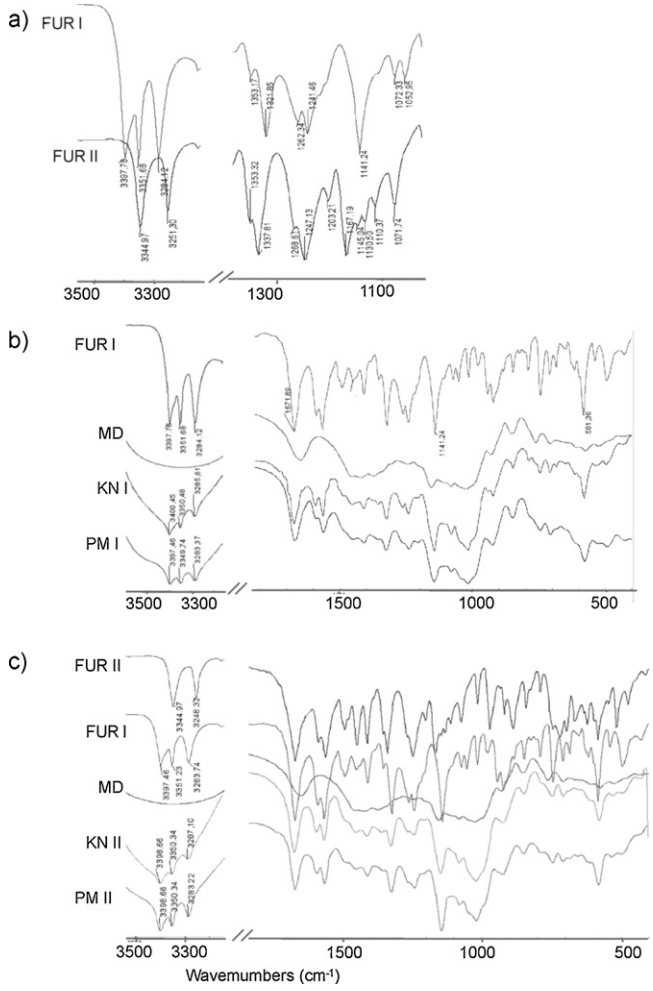

Fig. 4. FT-IR spectra of (a) FUR polymorphs, (b) FUR I:MD systems, and (c) FUR II:MD systems.

sulphonamide group and the aromatic ring interacted with the MD in the solid state. The spectrum of PM I corresponded simply to the superposition of the FT-IR spectra of the components.

For KN II, as well as for PM II (Fig. 4(c)), the FT-IR spectra corresponded to the superposition of the spectra of FUR I and MD, suggesting that a polymorphic transformation could have occurred by mechanical grinding during the preparation, as evidenced by ssNMR.

3.3.3. DSC and TGA

The DSC and TGA profiles of FUR I and II, and of the systems KN I, KN II, PM I and PM II, are shown in Fig. 5.

The DSC profile of FUR I showed three transitions: a weak endotherm at 136.8 °C, and a melting endotherm at 205.8 °C before an exotherm at 220.8 °C due to decomposition phenomena. In addition, no mass loss was seen in the TGA curve over the range 130–140 °C, indicating that the first endothermic event did not arise from desolvation and may have been associated with a polymorphic transformation at a temperature above 130 °C. The DSC profile of FUR II showed three transitions: an endotherm at 213.3 °C due to drug melting, and two exotherms at 215.9 and 218.1 °C attributed to the decomposition of the drug. The melting endotherms were very small for the FUR polymorphs because the compound decomposed at its melting temperature and the exotherm heat evolution dominated the profile. The TGA curves showed mass losses of up to 200 °C, which corresponded to the decomposition of the FUR polymorphs.

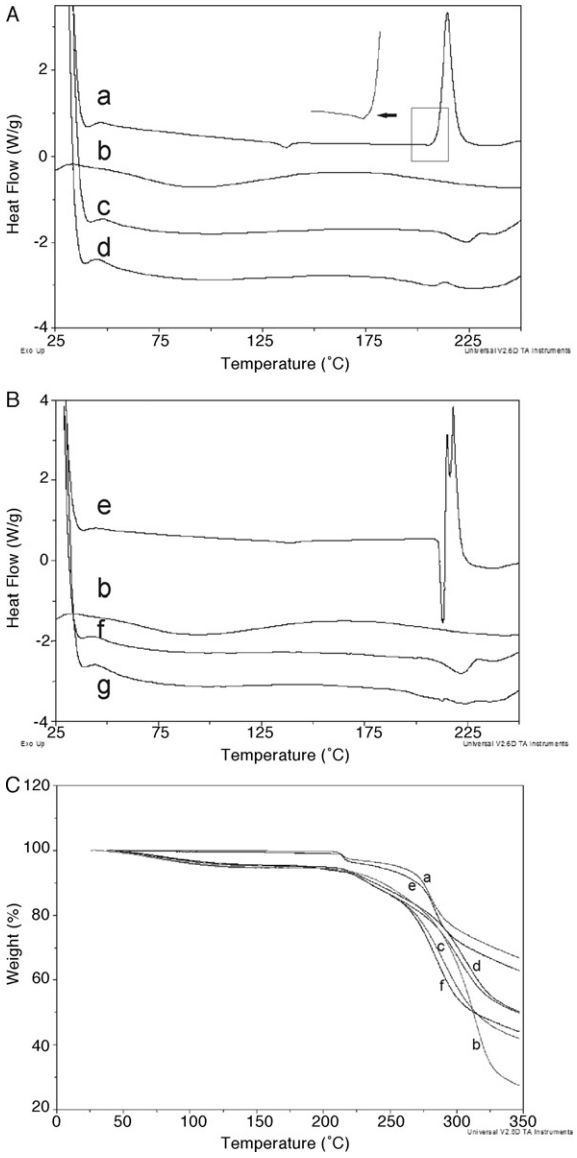

Fig. 5. DSC (A, B) and TGA (C) curves of (a) FUR I, (b) MD, (c) KN I, (d) PM I, (e) FUR II, (f) KN II, and (g) PM II.

Comparison of the DSC curves of both systems prepared by KN with those obtained by PM confirmed an interaction between the components. The DCS curve of the KN systems showed the complete disappearance of the FUR thermal events, indicating molecular interaction of the drug with the MD. Interestingly, in the PM the characteristic events observed for the individual components were found.

3.3.4. SEM

Supporting evidence for the complexation of FUR polymorphs I and II with MD was also obtained from SEM, with Fig. 6 showing the distinct morphological differences between the samples.

FUR I gave rise to the largest crystals, which appeared as hexagonal tubular crystals, whereas FUR II resulted in fine prisms with small elongations. The MD consisted of hollow spherical entities, with large particles containing smaller particles inside.

The images of KN I and KN II revealed a less ordered structure with compact and irregular arrangements. The original morphology of the raw materials disappeared, with it being impossible to differentiate between the two components. The drastic change in the particle shape and aspect of the solids obtained by KN was evidence

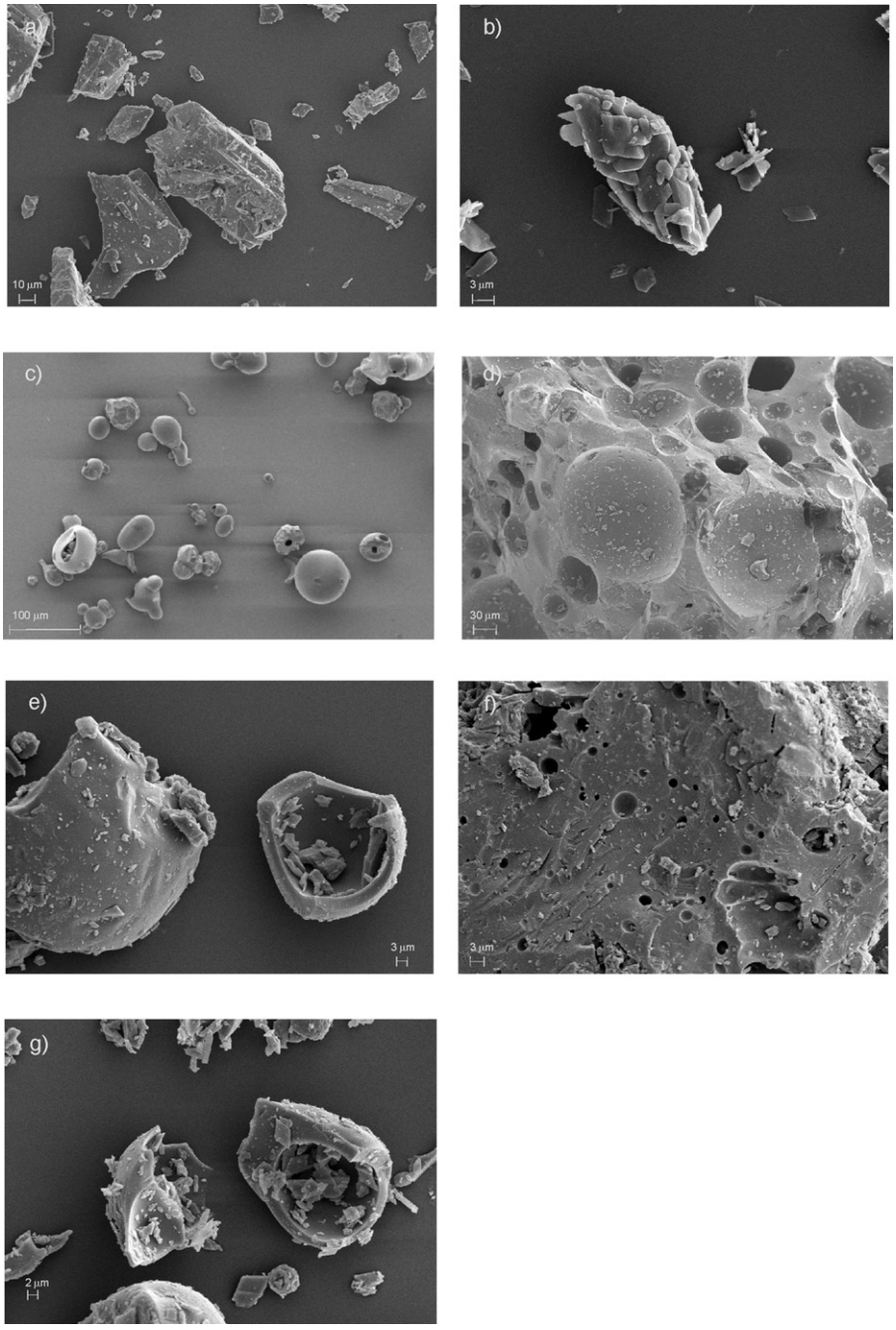

Fig. 6. Scanning electron microphotographs of (a) FUR I, (b) FUR II, (c) MD, (d) KN I, (e) PM I, (f) KN II, and (g) PM II.

of solid-state interactions and may indicate the presence of new solid phases. In contrast, SEM images of the PMs showed similarities with the components, revealing an absence of interactions in these solid systems.

3.3.5. XPRD

The XPRD patterns of the raw materials and the binary systems are shown in Fig. 7(a). The diffraction patterns of the FUR polymorphs I and II exhibited clear differences in terms of a series of intense and sharp peaks, confirming that they were different crystal forms. These results are in agreement with those reported previously (De Villiers et al., 1992; Matsuda & Tatsumi, 1990). In addition, the MD showed a hollow pattern, revealing its amorphous state.

The diffraction patterns corresponding to KN I and KN II showed a decrease in the degree of crystallinity. However, it was not possible to differentiate between systems I and II. Presumably, a phase conversion had occurred when the mixture of raw components was subjected to grinding in a mortar–pestle. On the other hand, the diffractograms of the PMs demonstrated the superimposition of the characteristic peaks of the FUR polymorphs and MD, although at a lower intensity due to dilution of the raw materials. These results correlated well with those of the FT-IR, thermal analysis and SEM studies.

3.4. Dissolution study

Fig. 7(b) displays the dissolution profiles of free FUR polymorphs I and II, and of the systems KN I, KN II, PM I and PM II. It can be seen that the dissolution behavior of KN I and II and the corresponding PMs displayed more dissolved drug and a faster dissolution rate,

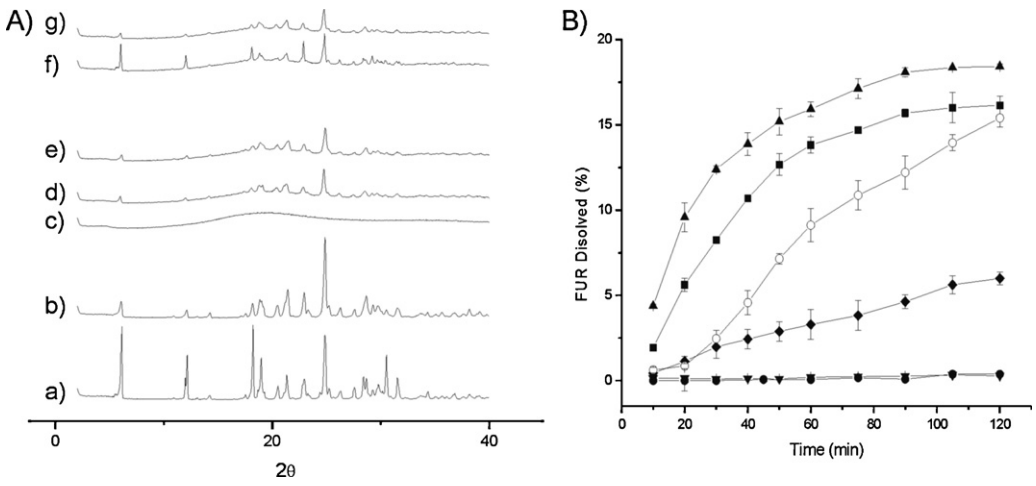

Fig. 7. (A) Powder X-ray diffraction patterns of (a) FUR I, (b) FUR II, (c) MD, (d) KN I, (e) KN II, (f) PM I, and (g) PM II. (B) Dissolution profiles in simulated gastric fluid of suitable quantities of each powder containing 50 mg of drug: FUR I (●), FURO II (▼), KN I (■), PM I (♦), KN II (▲) and PM II (○).

compared to the free polymorphs. Therefore some differences may have existed in the bioavailability of the two polymorphs.

It is interesting to note that KN I and II exhibited the greatest dissolution (although with similar dissolution curves), with KN II displaying a faster dissolution rate than KN I. This difference can be based on the FUR II behavior which showed the highest solubility in the phase solubility analysis, demonstrating the characteristic solid form obtained for each system, as evidenced by ^{13}C CP-MAS spectra and the ^{1}H–T_1 measurements. Our results indicated that the increase in drug solubility, resulting of the formation of supramolecular complexes, significantly favored the dissolution in simulated gastric fluid. The driving forces responsible for complex formation include electrostatic interactions, van der Waals contributions, hydrogen bonding, release of conformational strain and charge-transfer interactions. The increase in the amounts of drug dissolved allowed to suggest that there were interactions between each FUR polymorph and MD in the KN systems.

This performance is a bio-relevant fact since FUR is a drug classified into Class IV of the Biopharmaceutical Classification System (Granero et al., 2010). When used orally it is mainly absorbed from the stomach, and then the low solubility of the drug in this medium is the rate-determining step for its absorption. Considering that the dissolution characteristics are an important parameter to ensure the bioavailability of a drug product, these supramolecular complexes obtained by KN can be regarded as pharmaceutical alternatives to FUR, and may be a good method to develop more dose-efficient formulations.

The profiles of the PMs within the experimental conditions of the test demonstrated an increased dissolution rate in comparison to the free polymorphs. More specifically, significant differences in the dissolution properties between the two polymorphic forms became evident from the PMs, which reflected energetically dissimilar crystal forms. Despite the slower dissolution rate in relation to the KN systems, the PMs exhibited the most discriminating condition between the FUR forms I and II in simulated gastric fluid. In addition, the extent and rate of dissolution revealed that interactions between each FUR polymorph and MD may also be possible.

4. Conclusions

Our results confirm the formation of supramolecular complexes between FUR and MD, in solution and in solid state. The new complexes were characterized exhaustively using solubility studies, and the NMR, FT-IR, DSC, TGA, SEM and XRPD techniques. Based on these experiments, we can postulate that the complexes are new solid forms. Although it was difficult to spectroscopically characterize the new complexes in the solid state, probably due to the amorphous character of the MD and the KNs, the ^{1}H–T_1 relaxation NMR studies, DSC, TGA and SEM were decisive to be able to confirm the existence of the new solid forms.

The strategy based on the interaction between FUR and MD was demonstrated to have a positive effect on drug dissolution. This is encouraging, because the formation of the new complexes between the FUR polymorphs and MD might be of future use at on industrial scale for pharmaceutical formulations. Taking into account that FUR is incompletely absorbed after oral administration, the FUR:MD complexes provide an interesting alternative that is potentially useful for the preparation of pharmaceutical dosage products with a resultant positive impact on the oral bioavailability of FUR.

Acknowledgments

We are grateful for financial support from Fondo para la Investigación Científica y Tecnológica (FONCYT) Préstamo BID 1728/OC-AR PICT 1376, the Consejo Nacional de Investigaciones Científicas y Técnicas (CONICET) and the Secretaría de Ciencia y Técnica de la Universidad Nacional de Córdoba (SECyT-UNC). The assistance of Dr. Gloria M. Bonetto in performing NMR measurements and also her helpful discussions of the spectra are highly appreciated. We would like to thank Dr. Paul Hobson, native English speaker, for revision of the manuscript.

Appendix A. Supplementary data

Supplementary data associated with this article can be found, in the online version, at http://dx.doi.org/10.1016/j.carbpol.2013.01.055.

References

Bauer, M., Couteau, A., Monjanel, F., Pages, M., Videau, J. Y., & Yameogo, O. (2002). Effects of the physical characteristics of furosemide. *STP Pharma Pratiques*, *12*, 76–84.

Bayrakcı, M., Ertul, S., & Yılmaz, M. (2012). Solubilizing effect of the p-phosphonate calix[*n*]arenes towards poorly soluble drug molecules such as nifedipine, niclosamide and furosemide. *Journal of Inclusion Phenomena and Macrocyclic Chemistry*, *74*, 415–423.

Beyers, H., Malan, S. F., van der Watt, J. G., & de Villiers, M. M. (2000). Structure–solubility relationship and thermal decomposition of furosemide. *Drug Development and Industrial Pharmacy*, *26*, 1077–1083.

Brewster, M. E., & Loftsson, T. T. (2007). Cyclodextrins as pharmaceutical solubilizers. *Advanced Drug Delivery Reviews*, *59*, 645–666.

Brittain, H. G. (2009). *Polymorphism of pharmaceutical solids*. New York: Marcel Dekker.

Corralo Spada, J., Zapata Noreña, C. P., Ferreira Marczak, L. D., & Tessaro, I. C. (2012). Study on the stability of β-carotene microencapsulated with pinhão (*Araucaria angustifolia* seeds) starch. *Carbohydrate Polymers*, *89*, 1166–1173.

De Villiers, M. M., van der Watt, J. G., & Lotter, A. P. (1992). Kinetic study of the solid-state photolytic degradation of two polymorphic forms of furosemide. *International Journal of Pharmaceutics*, *88*, 275–283.

De Zordi, N., Moneghini, M., Kikic, I., Grassi, M., Del Rio Castillo, A., Solinas, D., et al. (2012). Applications of supercritical fluids to enhance the dissolution behaviors of furosemide by generation of microparticles and solid dispersions. *European Journal of Pharmaceutics and Biopharmaceutics*, *81*, 131–141.

Doherty, C., & York, P. (1988). Frusemide crystal forms; solids state and physicochemical analyses. *International Journal of Pharmaceutics*, *47*, 141–155.

Dokic, P., Jakovljevic, J., & Dokic-Baucal, L. (1998). Molecular characteristics of maltodextrins and rheological behaviour of diluted and concentrated solutions. *Colloids and Surfaces A*, *141*, 435–440.

Dokic-Baucal, L., Dokic, P., & Jakovljevic, J. (2004). Influence of different maltodextrins on properties of O/W emulsions. *Food Hydrocolloids*, *18*, 233–239.

Geppi, M., Guccione, S., Mollica, G., Pignatello, R., & Veracini, C. A. (2005). Molecular properties of ibuprofen and its solid dispersions with Eudragit RL100 studied by solid state nuclear magnetic resonance. *Pharmaceutical Research*, *22*, 1544–1555.

Granero, G., Longhi, M., Mora, M., Junginger, H., Midha, K., Shah, V., et al. (2010). Biowaiver monographs for immediate release solid oral dosage forms: furosemide. *Journal of Pharmaceutical Science*, *99*, 2544–2556.

Gurrapu, A., Jukanti, R., Bobbala, S., Kanuganti, S., & Jeevana, J. (2012). Improved oral delivery of valsartan from maltodextrin based proniosome powders. *Advanced Powder Technology*, *23*, 583–590.

Harris, R. K. (1994). *Nuclear magnetic resonance spectroscopy*. London: Longman Scientific and Technical.

Higuchi, T., & Connors, K. A. (1965). Phase-solubility techniques. In C. N. Reilly (Ed.), *Advances in analytical chemistry and instrumentation* (pp. 117–212). New York: Wiley-Interscience.

Hilfiker, R. (Ed.). (2006). *Polymorphism in the pharmaceutical industry*. Weinheim, Germany: Wiley-VCH.

Khitrin, A. K., Fujiwara, T., & Akutsub, H. (2003). Phase-modulated heteronuclear decoupling in NMR of solids. *Journal of Magnetic Resonance*, *162*, 46–53.

Kumar, B. P., Subbarao Murthy, K. V. R., & Sahu, R. K. (2012). Formulation, in vitro-evaluation and solid state characterization of solid dispersion of Efaverenz. *Journal of Chemical and Pharmaceutical Sciences*, *5*, 35–41.

Latosinska, J. N., Latosinska, M., Medycki, W., & Osuchowicz, J. (2006). Molecular dynamics of solid furosemide (4-chloro-2-furfurylamino-5-sulfamoyl-benzoic acid) studied by NMR and DFT methods. *Chemical Physics Letters*, *430*, 127–132.

Matsuda, Y., & Tatsumi, E. (1990). Physicochemical characterization of furosemide modifications. *International Journal of Pharmaceutics*, *60*, 11–26.

Munoz-Celaya, A. L., Ortiz-García, M., Vernon-Carter, E. J., Jauregui-Rincón, J., Galindo, E., & Serrano-Carreón., L. (2012). Spray-drying microencapsulation of *Trichoderma harzianum* conidias in carbohydrate polymers matrices. *Carbohydrate Polymers*, *88*, 1141–1148.

Ponto, L. L., & Schoenwald, R. D. (1990). Furosemide (frusemide). A pharmacokinetic/pharmacodynamic review (Part II). *Clinical Pharmacokinetics*, *18*, 460–471.

Pudipeddi, M., & Serajuddin, T. M. (2005). Trends in solubility of polymorphs. *Journal of Pharmaceutical Science*, *94*, 929–939.

Reineccius, G. A. (1989). Carbohydrates for flavour encapsulation. *Food Technology*, *45*, 144–149.

Shahidi, F., & Han, X. Q. (1993). Encapsulation of food ingredients. *Critical Reviews in Food Science and Nutrition*, *33*, 501–547.

Snider, D. A., Addicks, W., & Owens, W. (2004). Polymorphism in generic drug product development. *Advanced Drug Delivery Reviews*, *56*, 391–395.

Soini, H., Stefansson, M., Riekkola, M., & Novotny, M. (1994). Maltooligosaccharides as chiral selectors for the separation of pharmaceuticals by capillary electrophoresis. *Analytical Chemistry*, *66*, 3477–3484.

Sweetman, S. (Ed.). (2009). *Martindale: The complete drug reference*. London, UK/Greenwood Village, Colorado: Pharmaceutical Press, Thomson/Micromedex (Electronic version)

Vlachou, M., & Papaioannou, G. (2003). Preparation and characterization of the inclusion complex of furosemide with hydroxypropyl-β-cyclodextrin. *Journal of Biomaterials Applications*, *17*, 197–206.

Wang, J., & Wang, L. (2000). Structures and properties of commercial maltodextrins from corn, potato and rice starches. *Starch-Starke*, *52*, 296–304.